Letter

Contributions from ultraperipheral collisions to the forward rapidity gap distribution in *p*Pb collisions at the CERN Large Hadron Collider at $\sqrt{s_{NN}} = 8.16$ TeV

V. Guzey,[1] M. Strikman,[2] and M. Zhalov[1]

[1]*National Research Center "Kurchatov Institute", Petersburg Nuclear Physics Institute (PNPI), Gatchina 188300, Russia*

[2]*Pennsylvania State University, University Park, Pennsylvania 16802, USA*

(Received 10 May 2022; revised 13 July 2022; accepted 9 August 2022; published 22 August 2022)

In this Letter, we consider strong and electromagnetic (ultraperipheral) mechanisms in proton-nucleus coherent diffraction at the CERN Large Hadron Collider. We explicitly demonstrate the dominance of the latter and explain the CMS data on the forward rapidity gap distribution in *p*Pb collisions at $\sqrt{s_{NN}} = 8.16$ TeV. In particular, we provide simple estimates, which give a good, semiquantitative description of both magnitude and shape of the $\Delta\eta^F$ distribution in the Pomeron-proton topology. We also make predictions for the proton-oxygen run.

DOI: 10.1103/PhysRevC.106.L021901

Introduction and motivation. Diffraction in hadron scattering at high energies remains an active field of research. It is deeply connected to the nature of colorless exchanges with vacuum quantum numbers (Pomeron) in strong interactions and, more generally, small-x phenomena in quantum chromodynamics (QCD), important for tuning event generators needed for interpretation of results of ultrarelativistic heavy-ion scattering, and also relevant for cosmic ray physics. In experiments, diffractive events are characterized by large gaps in rapidity distributions of produced particles, which are defined as regions with no hadronic activity. To enhance sensitivity to such events and, in particular, to the so-called single diffractive dissociation, one can select events with the rapidity gaps in the most forward region of a detector; in proton-proton (pp) scattering such measurements have been performed at the CERN Large Hadron Collider (LHC) at $\sqrt{s_{NN}} = 7$ TeV [1,2].

The CMS Collaboration at the LHC for the first time measured the forward rapidity gap distribution in proton-Pb (pPb) collisions at $\sqrt{s_{NN}} = 8.16$ TeV [3]. It was found that for the Pomeron-proton topology, the EPOS-LHC, QGSJET II, and HIJUNG generators are at least a factor of 5 below the data. As a result, it was suggested that this discrepancy can be explained by a significant contribution of ultraperipheral photoproduction events mimicking the signature of diffractive processes.

Actually, this observation was already made in 2006 in Ref. [4], which showed that in coherent proton-nucleus (pA) diffraction the electromagnetic (ultraperipheral) contribution dominates the cross section for heavy nuclei. The purpose of this Letter is to generalize the results of Ref. [4] to the CMS experimental conditions and, in particular, to make predictions for the distribution in the forward rapidity gap $\Delta\eta^F$. Our predictions for the $\Delta\eta^F$ distribution in the studied case of the Pomeron-proton topology agree both in magnitude and shape with the results measured by the CMS Collaboration and, thus, confirm and quantify the essential role of ultraperipheral photoproduction in explanation of the CMS data.

We also make predictions for the case of proton-oxygen (pO) scattering.

Strong and electromagnetic mechanisms in pA coherent diffraction. The phenomenon of diffractive dissociation of protons in proton-nucleus scattering at high energies is a classic example of the composite structure of hadronic projectiles, which can be conveniently described within the framework of cross-section fluctuations [5–9]. In this approach, the cross section of pA coherent diffraction dissociation, $p + A \to X + A$, can be written in the following form:

$$\sigma_{pA}^{\rm diff}(s) = \int d^2\vec{b}\left[\int d\sigma P_p(\sigma)\left|\Gamma_A(\vec{b})\right|^2 - \left|\int d\sigma P_p(\sigma)\Gamma_A(\vec{b})\right|^2\right], \tag{1}$$

where s is the total proton-nucleus energy squared per nucleon. Here $\Gamma_A(\vec{b})$ is the nuclear scattering amplitude in representation of the impact parameter $\vec{b}$, which in the limit of high energies and large A (heavy nucleus) is usually expressed in the eikonal form

$$\Gamma_A(\vec{b}) = 1 - e^{-\frac{\sigma}{2}T_A(\vec{b})}, \tag{2}$$

where $T_A(\vec{b}) = \int dz\rho_A(\vec{r})$, with $\rho_A(\vec{r})$ being the nuclear density [10] normalized to the number of nucleons A. The $\Gamma_A(\vec{b})$ amplitude sums multiple interactions with target nucleons and captures the effect of nuclear shadowing leading to a dramatic suppression of the proton-nucleus cross section.

Published by the American Physical Society under the terms of the Creative Commons Attribution 4.0 International license. Further distribution of this work must maintain attribution to the author(s) and the published article's title, journal citation, and DOI. Funded by SCOAP³.

The distribution $P_p(\sigma)$ describes cross-section fluctuations of the proton and gives the probability for the proton to fluctuate into a hadronic configuration interacting with target nucleons with the cross section σ. In general, $P_p(\sigma)$ should be modeled (see, e.g., Refs. [7,9]). However, in the case of diffraction dissociation, the detailed information on the shape of $P_p(\sigma)$ is not needed since one can use the general property that $P_p(\sigma)$ is peaked around $\sigma_{pp}^{\rm tot}(s) = \langle\sigma\rangle \equiv \int d\sigma P_p(\sigma)\sigma$. Thus, expanding Eq. (1) around $\langle\sigma\rangle$, one obtains [6]

$$\sigma_{pA}^{\rm diff}(s) = \frac{\omega_\sigma(s)\langle\sigma\rangle^2}{4}\int d^2\vec{b}[T_A(\vec{b})]^2 e^{-\langle\sigma\rangle T_A(\vec{b})}, \tag{3}$$

where $\omega_\sigma(s) = \langle\sigma^2\rangle/\langle\sigma\rangle^2 - 1$ quantifies the dispersion of cross-section fluctuations of the proton. At $\sqrt{s} = \sqrt{s_{NN}} = 8.16$ TeV, we use the COMPETE parametrization [11] giving $\langle\sigma\rangle = \sigma_{pp}^{\rm tot}(s) = 98.6$ mb and a simple interpolation from fixed-target to energies available at the Tevatron and further extrapolation to energies available at the LHC giving $\omega_\sigma(s) = 0.092 \pm 0.050$ [9]. The spread in the values of $\omega_\sigma(s)$ reflects the theoretical uncertainty in modeling $P_p(\sigma)$. Note that the accuracy of approximating Eq. (1) by Eq. (3) is better than the significant uncertainty of $\omega_\sigma(s)$, which is amplified by its extrapolation from energies available at the Tevatron to those available at the LHC and which dominates the uncertainty of the predicted values of $\sigma_{pA}^{\rm diff}(s)$.

It was explained in Ref. [4] that a competing reaction mechanism leading to the same final state, $p + A \to p + \gamma + A \to X + A$, is provided by the electromagnetic contribution corresponding to ultraperipheral pA scattering. In this case, proton and Pb beams pass each other at large impact parameters and, hence, short-range strong interactions are suppressed. Instead, the relativistic heavy-ion beam serves as an intensive source of quasireal photons, which interact with the proton. In the equivalent photon (Weizsäcker-Williams) approximation, the corresponding cross section reads [12,13]

$$\sigma_{pA}^{\rm e.m.}(s) = \int_{\omega_{\rm min}}^{\omega_{\rm max}} \frac{d\omega}{\omega} N_{\gamma/A}(\omega)\sigma_{\gamma p}^{\rm tot}(s_{\gamma p}), \tag{4}$$

where $N_{\gamma/A}(\omega)$ is the photon flux, ω is the photon energy, $\sigma_{\gamma p}^{\rm tot}(s_{\gamma p})$ is the total photon-proton cross section, and $s_{\gamma p}$ is the total invariant photon-proton energy squared. The integration limits can be estimated as follows. In the laboratory frame, the minimal photon energy corresponding to photoexcitation of the lowest inelastic state is $\omega_{\rm min} = (M_\Delta^2 - m_p^2)/[4m_p\gamma_L(p)]$, where M_Δ and m_p are the masses of $\Delta(1232)$ and the proton, respectively, and $\gamma_L(p) = E_p/m_p$ is the Lorentz factor of the proton beam with energy E_p. The maximal photon energy is usually estimated as $\omega_{\rm max} = \gamma_L(A)/R_A$, where R_A is the nucleus effective radius and $\gamma_L(A) = E_A/m_p$ is the Lorentz factor of the nucleus beam with energy E_A.

For the photon flux, we use the approximate expression corresponding to the pointlike source with the electric charge Z:

$$N_{\gamma/A}(\omega) = \frac{2Z^2\alpha_{\rm e.m.}}{\pi}\left(\xi K_0(\xi)K_1(\xi) - \frac{\xi^2}{2}\left[K_1^2(\xi) - K_0^2(\xi)\right]\right), \tag{5}$$

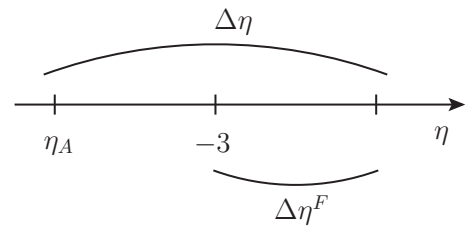

FIG. 1. Sketch of the definition of the rapidity gap size $\Delta\eta^F$ in the Pomeron-proton topology at the CMS Collaboration.

where $\alpha_{\rm e.m.}$ is the fine-structure constant; $K_{0,1}$ are modified Bessel functions of the second kind; and $\xi = [\omega/\gamma_L(A)]b_{\rm min}$, with $b_{\rm min} = 1.15R_A$ and $R_A = 1.145A^{1/3}$ fm. With these parameters, Eq. (5) reproduces with a 5% precision a more accurate calculation of the photon flux taking into account the suppression of strong interactions at $|\vec{b}| \leqslant b_{\rm min}$ [14]. This estimate of the accuracy of Eq. (5) is based on the analysis of Ref. [14] and also includes the effect of the use of different nuclear density distributions.

For the total photon-proton cross section, we use the Donnachie and Landshoff fit [15]

$$\sigma_{\gamma p}^{\rm tot}(s)/{\rm mb} = 0.0677 s_{\gamma p}^{0.0808} + 0.129 s_{\gamma p}^{-0.4525}, \tag{6}$$

where $s_{\gamma p} = 4\omega E_p + m_p^2$.

Employing the input specified above and using Eqs. (3) and (4), we obtain the following results for the strong and electromagnetic (ultraperipheral) contributions to the cross section of pPb coherent diffraction at $\sqrt{s_{NN}} = 8.16$ TeV:

$$\begin{aligned}\sigma_{pA}^{\rm diff}(s) &= 7.4 \pm 4.0 \text{ mb},\\ \sigma_{pA}^{\rm e.m.}(s) &= 450 \pm 23 \text{ mb}.\end{aligned} \tag{7}$$

These values agree with those of Ref. [4] (the correct predictions for the electromagnetic contribution are given in the Erratum to that paper) and of Ref. [16]. The uncertainty in the predicted value of $\sigma_{pA}^{\rm e.m.}(s)$ comes from the uncertainty in $N_{\gamma/A}(\omega)$.

Predictions for the strong and electromagnetic contributions differential in $\Delta\eta^F$. In proton-nucleus coherent diffraction, the size of the rapidity gap between the intact nucleus and the diffractively produced system X is

$$\Delta\eta = -\ln\xi_X, \tag{8}$$

where $\xi_X = M_X^2/s$ is a variable commonly used in diffraction and M_X is the mass of the state X. In the case of Pomeron-proton topology, the CMS Collaboration has defined $\Delta\eta^F$ as the distance from $\eta = -3$ to the lower edge of the last nonempty η bin [3]. Since the elastically scattered nucleus corresponds to $\eta_A = -(1/2)\ln(4E_A^2/m_p^2) = \ln(2E_A/m_p) = -8.6$ (in the CMS coordinate system, the direction of the proton beam in pPb collisions defines positive rapidity), we obtain

$$\Delta\eta^F = \Delta\eta - (8.6 - 3) = \Delta\eta - 5.6. \tag{9}$$

This is illustrated in Fig. 1. It should be compared to the definition of the ATLAS Collaboration in the pp case at $\sqrt{s_{NN}} = 7$ TeV, $\Delta\eta^F = \Delta\eta - 4$ [1].

Turning to Eq. (3) and recalling that the cross section of diffraction dissociation on the proton (nucleon) at the momentum transfer $t = 0$ is related to the dispersion of cross-section fluctuations [5],

$$\frac{d\sigma_{pp}^{\rm diff}(t=0)}{dt} = \frac{1}{16\pi}(\langle\sigma^2\rangle - \langle\sigma\rangle^2) = \frac{\omega_\sigma(s)\langle\sigma\rangle^2}{16\pi}, \quad (10)$$

Eq. (3) can be rewritten in the following form:

$$\sigma_{pA}^{\rm diff}(s) = \frac{d\sigma_{pp}^{\rm diff}(t=0)}{dt} 4\pi \int d^2\vec{b}[T_A(b)]^2 e^{-\langle\sigma\rangle T_A(b)}. \quad (11)$$

Making the common assumption of an exponential momentum transfer t dependence, $d\sigma_{pp}^{\rm diff}/dt = e^{-B(s)|t|} d\sigma_{pp}^{\rm diff}(t = 0)/dt$, we can express the proton-nucleus diffractive cross section as a product of the t-integrated proton-proton diffractive cross section $\sigma_{pp}^{\rm diff}(s)$ and the nuclear factor,

$$\begin{aligned}\sigma_{pA}^{\rm diff}(s) &= \sigma_{pp}^{\rm diff}(s) 4\pi B(s) \int d^2\vec{b}[T_A(b)]^2 e^{-\langle\sigma\rangle T_A(b)} \\ &= (2.4 \pm 0.16)\, \sigma_{pp}^{\rm diff}(s). \end{aligned} \quad (12)$$

In the second line of Eq. (12), we used that $B(s) \approx B_{\rm el} + 2\alpha'_{\boldsymbol{P}} \ln(m_p^2/M_X^2) \approx 15 \pm 1$ GeV^{-2} for $40 \leqslant M_X \leqslant 300$ GeV at $\sqrt{s_{NN}} = 8.16$ TeV. This estimate is based on the experimental results for the slope of the t dependence of the elastic pp cross section $B_{\rm el} \approx 20 \pm 0.5$ GeV^{-2} [11] and the general dependence of the slope of single diffractive dissociation on M_X^2 in Regge phenomenology with $\alpha'_{\boldsymbol{P}} \approx 0.25$ GeV^{-2}; the used range of M_X corresponds to $1 \leqslant \Delta\eta^F \leqslant 5$.

Equation (12) has a transparent probabilistic interpretation: the process of diffractive dissociation with the cross section $d\sigma_{pp}^{\rm diff}(t = 0)/dt = B(s)\sigma_{pp}^{\rm diff}(s)$ takes place coherently on nuclear target nucleons, which are distributed in the transverse plane with the probability $[T_A(b)]^2$; the probability to maintain nuclear coherence, i.e., the probability not to have inelastic interactions within the nuclear volume, is given by the standard Glauber model factor $e^{-\langle\sigma\rangle T_A(b)}$.

This factorization (decoupling) of diffractive dissociation on the nucleon from the effect of nuclear suppression, which does not depend on the diffraction, allows for a simple generalization to the case of cross section differential in the produced diffractive mass M_X (the variable ξ_X) or the size of the rapidity gap $\Delta\eta^F$ [see Eqs. (8) and (9)]. Indeed, taking advantage of a simple connection between $\sigma_{pA}^{\rm diff}(s)$ and $\sigma_{pp}^{\rm diff}(s)$ and neglecting a weak dependence on ξ_X of the slope $B(s)$ and the nuclear factor in Eq. (12), we can generalize Eq. (12) to the form differential in $\Delta\eta^F$,

$$\frac{d\sigma_{pA}^{\rm diff}}{d\Delta\eta^F} = (2.4 \pm 0.16)\, \frac{d\sigma_{pp}^{\rm diff}}{d\Delta\eta^F}. \quad (13)$$

Finally, without resorting to a particular model for $d\sigma_{pp}^{\rm diff}/d\Delta\eta^F$, we use the ATLAS result that $d\sigma_{pp}^{\rm diff}/d\Delta\eta^F \approx 1$ mb for $\Delta\eta^F \geqslant 3$ [1] and thus arrive at the following estimate,

$$\frac{d\sigma_{pA}^{\rm diff}}{d\Delta\eta^F} \approx 2.4 \pm 1.3 \text{ mb}. \quad (14)$$

The uncertainty in this estimate comes from the significant uncertainty in the value of $\omega_\sigma(s)$ discussed above [see the first line of Eq. (7)]. Note that Eq. (14) becomes less accurate for small values of the rapidity gap since, in the pp case for $\Delta\eta^F < 2$, nondiffractive processes dominate and $d\sigma_{pp}^{\rm diff}/d\Delta\eta^F$ begins to rapidly grow (see the CMS data point at $\Delta\eta^F < 1$ in Fig. 2 below).

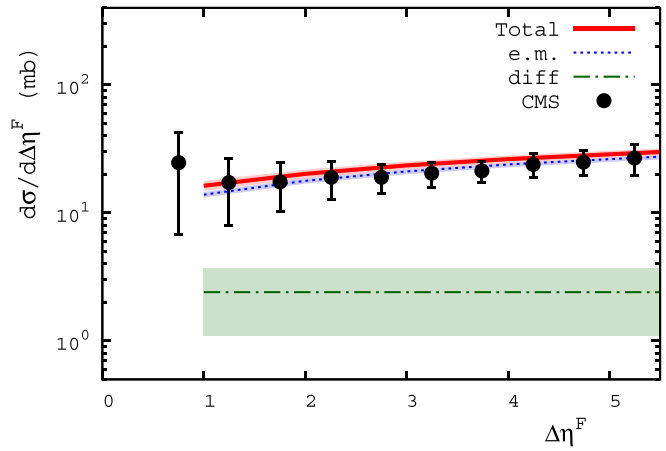

FIG. 2. The strong ("diff"), electromagnetic ("e.m."), and total ("Total") contributions to the cross section of pPb coherent diffraction as a function of $\Delta\eta^F$ at $\sqrt{s_{NN}} = 8.16$ TeV. The preliminary CMS data [3] are shown by solid circles with error bars.

The estimate of Eq. (14) semiquantitatively agrees with predictions of the EPOS-LHC, QGSJET II, and HIJUNG generators shown in Fig. 2 of Ref. [3]. In particular, for $\Delta\eta^F \geqslant 2$, it agrees on a logarithmic scale with the approximately constant predictions of QGSJET II, $d\sigma/d\Delta\eta^F \approx 2$ mb, and of EPOS-LHC and HIJING, $d\sigma/d\Delta\eta^F \approx 4$ mb. For $\Delta\eta^F < 2$, results of these event generators tend to somewhat increase.

Turning to Eq. (4), we notice that the photon energy required to excite the diffractive mass M_X is $\omega = (M_X^2 - m_p^2)/[4m_p\gamma_L(p)] \approx M_X^2/[4m_p\gamma_L(p)]$ for sufficiently large M_X. Therefore,

$$\frac{d\omega}{\omega} = d\ln M_X^2 = d\Delta\eta^F. \quad (15)$$

It allows us to rewrite Eq. (4) in the form differential in $\Delta\eta^F$ as

$$\frac{d\sigma_{pA}^{\rm e.m.}}{d\Delta\eta^F} = N_{\gamma/A}[\omega(\Delta\eta^F)]\sigma_{\gamma p}^{\rm tot}(s_{\gamma p}), \quad (16)$$

where the photon energy corresponds to the given $\Delta\eta^F$, i.e., to the given M_X [see Eqs. (8) and (9)]. The resulting values of $d\sigma_{pA}^{\rm e.m.}/d\Delta\eta^F$ as a function of $\Delta\eta^F$ in the $1 \leqslant \Delta\eta^F \leqslant 5$ interval are given in Table I (second column). The 5% uncertainty comes from the uncertainty in the photon flux $N_{\gamma/A}(\omega)$. In the last column of the table, we give a sum of the electromagnetic and strong interaction contributions (total cross section), where the respective uncertainties have been added in quadrature.

In a graphical form our results are summarized in Fig. 2. It shows the strong (green dot-dashed curve labeled "diff"), electromagnetic (blue dotted curve labeled "e.m."), and total (the sum of the former two given by the red solid curve labeled "Total") contributions to the cross section of

TABLE I. The contribution of the electromagnetic (ultraperipheral) mechanism to pPb coherent diffraction, $d\sigma_{pA}^{\rm e.m.}/d\Delta\eta^F$, and a sum of the electromagnetic and strong interaction contributions (total cross section), $d\sigma_{pA}/d\Delta\eta^F$, as a function of the rapidity gap size $\Delta\eta^F$.

$\Delta\eta^F$	$d\sigma_{pA}^{\rm e.m.}/d\Delta\eta^F$ (mb)	$d\sigma_{pA}/d\Delta\eta^F$ (mb)
1	13.9 ± 0.70	16.3 ± 1.48
2	17.8 ± 0.89	20.2 ± 1.58
3	21.1 ± 1.06	23.5 ± 1.68
4	23.9 ± 1.20	26.3 ± 1.77
5	26.3 ± 1.32	28.7 ± 1.85

proton-lead (pPb) coherent diffraction as a function of $\Delta\eta^F$. The shaded bands represent uncertainties of our predictions detailed above; the band for the total cross section is obtained by adding in quadrature the uncertainties of the strong and electromagnetic contributions. The preliminary CMS data are shown by solid circles with error bars; we extracted them from Ref. [3] using the WEBPLOTDIGITIZER tool [17].

A comparison to the CMS results presented in Fig. 2 shows that our simple estimate reproduces rather well both the magnitude and the shape of the measured $\Delta\eta^F$ distribution, which exhibits a slow, monotonous increase from $d\sigma/d\Delta\eta^F \approx 20$ mb at $\Delta\eta^F = 1$ to $d\sigma/d\Delta\eta^F \approx 30$ mb at $\Delta\eta^F = 5$. Thus, we demonstrate that the ultraperipheral mechanism is responsible for the increase of $d\sigma/d\Delta\eta^F$ with an increase of $\Delta\eta^F$. Note that the $\Delta\eta^F < 1$ region, where $d\sigma_{pp}^{\rm diff}/d\Delta\eta^F$ begins to rapidly grow, corresponds to nondiffractive processes and, hence, is outside of the range of applicability of our approach.

It is important to note that our estimate of $d\sigma_{pA}^{\rm e.m.}/d\Delta\eta^F$ is based on the assumption that it receives contributions from all M_X comprising the total photon-proton cross section and, hence, should be considered as an upper limit. A more accurate account of the ultraperipheral contribution to $d\sigma/d\Delta\eta^F$ should include modeling of the mass spectrum in photon-proton scattering and the influence of the detector acceptance, which is beyond the scope of our work.

While the aim of this Letter was to capture the bulk of physical effects explaining the CMS results in a semiquantitative way, our calculations can be improved along several lines, in particular, in an estimate of the strong interaction mechanism of coherent diffraction. However, since it gives a subleading contribution, these refinements will not significantly affect the resulting total $\Delta\eta^F$ distribution.

Predictions for proton-oxygen run. One can readily extend our predictions to proton-oxygen (pO) scattering at $\sqrt{s_{NN}} = 9.19$ TeV. In this case, $\sigma_{pp}^{\rm tot}(s) = 100.6$ mb and $\omega_\sigma(s) = 0.086 \pm 0.050$, and we obtain [compare to Eq. (7)]

$$\sigma_{pO}^{\rm diff}(s) = 3.1 \pm 1.8 \text{ mb},$$
$$\sigma_{pO}^{\rm e.m.}(s) = 5.0 \pm 0.25 \text{ mb}. \quad (17)$$

One can see that the strong interaction and electromagnetic contributions have comparable magnitudes for oxygen because of a 100 times smaller photon flux compared to Pb. As a result, the electromagnetic contribution constitutes a 15–30% correction to the $\Delta\eta^F$ distribution. At the same time, this gives an opportunity to measure the cross section of soft pO diffraction, which is strongly suppressed by nuclear shadowing compared to the impulse approximation.

Summary. In summary, we have shown that a straightforward extension of the results of Ref. [4] can explain the CMS data on the forward rapidity gap distribution in pPb collisions at $\sqrt{s_{NN}} = 8.16$ TeV. Notably, we have explicitly demonstrated the dominance of the electromagnetic (ultraperipheral) mechanism in the Pomeron-proton topology, which provides a good, semiquantitative description of both the magnitude and the shape of the measured $\Delta\eta^F$ distribution.

Acknowledgments. The research of M.S. was supported by the U.S. Department of Energy, Office of Science, Office of Nuclear Physics, under Grant No. DE-FG02-93ER40771. M.S. thanks the Theory Division of CERN for hospitality while this work was done.

[1] G. Aad *et al.* (ATLAS Collaboration), Eur. Phys. J. C **72**, 1926 (2012).
[2] V. Khachatryan *et al.* (CMS Collaboration), Phys. Rev. D **92**, 012003 (2015).
[3] D. Sosnov (CMS Collaboration), Phys. Part. Nucl. **53**, 393 (2022); Report No. CMS-PAS-HIN-18-019.
[4] V. Guzey and M. Strikman, Phys. Lett. B **633**, 245 (2006); Erratum: **663**, 456 (2008).
[5] M. L. Good and W. D. Walker, Phys. Rev. **120**, 1857 (1960).
[6] L. Frankfurt, G. A. Miller, and M. Strikman, Phys. Rev. Lett. **71**, 2859 (1993).
[7] B. Blättel, G. Baym, L. L. Frankfurt, H. Heiselberg, and M. Strikman, Phys. Rev. D **47**, 2761 (1993).
[8] L. Frankfurt, V. Guzey, and M. Strikman, J. Phys. G: Nucl. Part. Phys. **27**, R23 (2001).
[9] L. Frankfurt, V. Guzey, A. Stasto and M. Strikman, arXiv:2203.12289 [Rep. Prog. Phys. (to be published)].
[10] H. De Vries, C. W. De Jager, and C. De Vries, At. Data Nucl. Data Tables **36**, 495 (1987).
[11] P. A. Zyla *et al.* (Particle Data Group), Prog. Theor. Exp. Phys. **2020**, 083C01 (2020).
[12] G. Baur, K. Hencken, D. Trautmann, S. Sadovsky, and Y. Kharlov, Phys. Rep. **364**, 359 (2002).
[13] A. J. Baltz, G. Baur, D. d'Enterria, L. Frankfurt, F. Gelis, V. Guzey, K. Hencken, Y. Kharlov, M. Klasen, S. R. Klein *et al.*, Phys. Rep. **458**, 1 (2008).
[14] V. Guzey and M. Zhalov, J. High Energy Phys. 02 (2014) 046.
[15] A. Donnachie and P. V. Landshoff, Phys. Lett. B **296**, 227 (1992).
[16] V. P. Gonçalves, R. P. da Silva and P. V. R. G. Silva, Phys. Rev. D **100**, 014019 (2019).
[17] https://automeris.io/WebPlotDigitizer/